An *in vitro* pilot study of the abutment stability during loading in virgin and fatigue-loaded conical dental implants using synchrotron-based radiography

T. Rack, S. Zabler, A. Rack, H. Riesemeier, K. Nelson

Keywords: X-ray imaging; dental implants; digital radiography; titanium, X-ray phase-contrast.

ABSTRACT

The implant-abutment connection of a two-piece dental implant depicts a complex micro-mechanical behavior: a micro-gap is evident at the implant-abutment interface, even in the virgin state. Its width varies when external mechanical load is applied. High resolution synchrotron-based radiography in combination with hard X-ray phase contrast to image this gap and estimate its size is deployed. The study involves commercially available implants with different internal conical implant-abutment connections. A comparison between virgin implants and the fatigue loaded implants underlines that fatigue extends the size of the micro-gap and increases the ability of micromovement. The cone angle of the connection influences the stability of the abutment. Cyclic loading at medium force (120 N) hence induces plastic deformation of the titanium implant.

1. Introduction

Two-piece dental implants, commonly used, feature a mating zone termed implant–abutment connection (IAC). The mating zone utilized in all two-piece implants can be subdivided into two principles: a horizontal butt-joint connection or a conical connection.[1] Research concerning the IAC has focused on its geometric precision, [2,3] its mechanical stability [4-9] and the risk of leakage at the implant-abutment interface. [10-16] Conical connections have been proposed to improve the resistance against mechanical failure of the IAC.[6,8] Technical complications concerning the abutment/abutment screw or the implant occur in 5 - 27 % of the implants placed with a doubling of the failure rate after 5 years in function.[17-19]

IAC´s are screwed joints that are exposed to dynamic loading with axial forces up to 450 N [20] and extra-axial forces with angles of up to 90 °. [21,22] Various scenarios to simulate long-term dynamic loading for the evaluation of fatigue and fracture strength of an implant have mounted to the DIN ISO Standard 14801:2003.[23]

To date the impact of fatigue loading on the implant-abutment interface of conical IAC´s has only been investigated by quantifying and visualizing the size of the micro-gap in unloaded specimens using synchrotron-based micro-tomography.[24] It has shown that there is no surface contact but only focal contact of the assembled components leading to a micro-gap even in assembled virgin implant-abutment connections that have not experienced any load application. [24,25]

For *in vitro* visualization of a micro-gap at the IAC of implants with conical mating surfaces monochromatic hard X-ray synchrotron radiography can be employed.[24,26] In comparison to conventional radiography based on x-ray tubes, images recorded with hard synchrotron light feature higher spatial resolution and material contrast. [27,28] Using phase-contrast radiography even sub-micrometer gaps can be detected whereby their size is quantified through comparison with numerical simulations [26] allowing besides visualization the quantification of the micro-gap in fatigue loaded conical implant-abutment connections during static load application. This study investigates and compares the effect of fatigue loading on the implant-abutment interface of conical implants with varying conus length and angle.

2. Materials and methods

2.1. Dental implant and test stand

All implants and abutments were purchased from the manufacturers. A pair of implants with abutments from three different dental implant systems (Table 1) with conical IAC were assembled and screw-tightened with a system-specific torque and ratchet. According to EN ISO Standard 14801:2003 individually fabricated steel-balls (Ø 10 mm) were perforated on one side and glued to the abutments with a two-component Methyl-Methacrylate-based adhesive (X60; HBM Germany, Darmstadt).

The implant–abutment assemblies were embedded in 15 mm brass cylinders (Fraunhofer Institut Werkstoffmechanik, Freiburg, Germany) according to EN ISO Standard 14801:2003 [25]. One implant-abutment assembly from each pair was fatigue loaded according to the ISO Standard 14801:2003 by the Fraunhofer Institute, Freiburg in a dry environment (5 x 10^6 cycles, 12-120 N amplitude, R=0.1 force ratio and f=15 Hz frequency at 30° inclination) prior to the radiographic measurements.

The brass cylinders with the implant–abutment assemblies were tightened into an individually fabricated steel test stand as described, [25] and a static extra-axial force

was applied. The constant force was thus applied at an standard angle of 30° (nominal 200 N) and 90° (nominal 30 N and 100 N) wi th respect to the implant axis onto the ball. Prior to loading each sample was measured without load. The force application was monitored using a digital force gauge model SH-500 [PCE-group OHG (serial No. 5808062790)]. [25] For the fatigue loaded specimen the static force was applied collinear to the fatigue force-vector which has been marked by a notch in the brass cylinder.

2.2 Synchrotron radiography with absorption and inline x-ray phase-contrast

High-resolution radiographs were acquired at the BAMline on the BESSY-II light source (Helmholtz Zentrum Berlin, Germany) (Rack et al., 2008). To penetrate the 3 - 4 mm Titanium, a photon energy of 50 keV was selected through the setting of a double-multilayer monochromator. Radiographic projection images were recorded by an indirect detector employing an effective pixel size of 0.45 µm (1.7 mm x 1.1 mm field of view). Radiography of each specimen was achieved with a propagation distance between sample and detector of either 4.5 or 74 cm. Owing to the limited field of view of a high-resolution indirect X-ray pixel detector, only a region of interest of the specimen is investigated. [25] As the length of the implant-abutment interface varies between 0.7- 2.3 mm and because the height of the synchrotron beam is limited as well, generally two images were acquired for each side of each implant and later merged in order to illustrate the complete gap. Despite the small pixel size the spatial detector resolution was around 4 µm in absorption mode and ~14 µm in phase-contrast, due to smearing by the demagnified X-ray source. The raw images were corrected for the camera's dark current then normalized by flatfield images. Line scans across the IAC were extracted with the software ImageJ (National Institute of Mental Health, Bethesda, Maryland, USA). To ensure a good signal and to compensate for photon noise, a line width of 200 pixels (~80 µm) was chosen, each profile having a length of 0.4 mm.

2.3 Quantitative characterization of the micro-gap at the IAC

Recent work by Zabler et al. has shown that micro-gaps at the IAC can be detected and quantified down to a gap width of the order of 0.1 µm by phase-contrast X-ray

radiography. Subsequently estimating the exact width is possible by further matching line-profiles across the gap to interference patterns obtained through numerical forward simulations of the partially coherent x-ray propagation across a virtual IAC. [26] For gaps larger than 5 µm – with the setup described above – it is also possible to determine the gap width from x-ray absorption radiographs where they show up as a discontinuity in attenuation profiles.

Results

Measurement of the geometric dimensions of the conical IAC´s including the length of the mating zone of the implant and abutment and the angle of the conus was performed using the radiographic images (Table 1). The region of interest of the data acquisition within the IAC is shown in Figure 1 and the results are listed in Table 2.

Load condition: 0 N

The virgin implant-abutment interface of each system were radiographed prior to static load application, they showed a micro-gap varying between 0.1 and 11 µm. The fatigue loaded samples showed a considerably larger gap between implant and abutment (0.1 - 31 µm). As depicted in Figure 2b the most significant changes were seen in the system Ankylos plus (ANP02). The gap in position A of ANP02 increased by a factor 100x compared to the virgin implant (ANP01)(Figure 2a), namely from 0.32 µm up to 31 µm, and a fissure is visible in the upper edges (A and AF) of the implant (Figure 2c).

Ankylos c/x IAC demonstrated a decreased micro-gap after fatigue loading. After fatigue loading (AN02) the maximum micro-gap value was smaller (4 µm) compared to the sample of the virgin implant (AN01) with a maximum gap size of 11 µm.

The size of the micro-gap of the fatigue loaded BoneLevel IAC (ST02: 0.8 µm) compared to the virgin IAC (ST01: 0.4 µm) increased 100 %.

Load condition: 30 N, 90°

Static load of 30 N was applied perpendicular (90°) to the implant axis and the resulting gap was measured. The implants of the Ankylos c/x system (AN01 and AN02) showed an increase of their micro-gap on the side of load application up to 12 µm in the coronal portion (AF) of the IAC and 0.1 µm in the most apical part of the IAC (BF).

An augmentation of the gap size in fatigue loaded IAC (ANP02) compared to the IAC of the virgin implant (ANP01) was seen in the system Ankylos plus (ANP). Regardless of their pretreatment the gap increased tenfold when a load of 30 N was applied with a maximum of 32 µm.

The behaviour of the micro-gap of the virgin BoneLevel implant ST01 during horizontal loading has been described.[25] When horizontal load is applied the fatigue-loaded sample (ST02) a 40 % increase of the size of the micro-gap up to 1.8 µm can be detected. Noticeable is that the micro-gap shows a parallel opening with almost the same value in the coronal (AF) and the apical (BF) portion of the IAC.

Load condition: 100 N, 90°

At 100 N of static load 90° to the implant axis the tendency of the gap width perpetuates. Ankylos c/x (AN01, AN02) doubles its gap size to 28 µm when load is increased from 30 N to 100 N. Again this is independent of the pretreatment of the implants. Along the gap no point contact between the abutment and the implant can be seen. The IAC opposite of the side of load application shows a complete closure of the gap in the coronal region (A) but an opening at the apex (B) with 4.6 µm in AN01 and 2.5 µm in AN02.

The gap of the fatigue-loaded IAC of Ankylos plus (ANP02) shows an angular micro-gap formation of 36 µm in position AF and a point contact in BF (Figure 3a). Whereas the virgin implant shows no point contact with an angular micro-gap opening of 18.5 µm in region AF and 0.1 µm in BF. A point contact can be seen at the most apical part of the loading side (BF) and at the top of the contralateral side (A) of load application only in the fatigue loaded implant (ANP02).

In the BoneLevel system the micro-gap opens almost parallel with a size of 10 - 14 µm (ST01) and 13 - 18 µm (ST02) from the apical to the coronal part of the IAC (Figure 3b).

Load condition: 200 N, 30°

Load of 200 N applied in a 30° angle to the virgin IAC Ankylos c/x (AN01) showed a gap opening at position AF to 24 µm, which was almost the same in the fatigue loaded implant (AN02: 22 µm). But the gap value on the side opposite to the side of force application of the fatigue-loaded sample (A) is fourfold higher (AN01: 0.7 µm;

AN02: 3 µm). No point contact between the abutment and implant can be seen in either sample anywhere in the radiographs of the IAC (Fig. 4a).
Ankylos plus (ANP02) shows approximately a threefold enhancement of the gap in position AF (9 µm) in respect to the same position in ANP01 (25 µm) with no point contact between the implant and abutment in any radiograph.
The IAC of BoneLevel is less sensitive to force applied in a 30° angle then to horizontal force application (Fig. 4b). The micro-gap size varies between 0.3 µm in the virgin implant (ST01) to 1 µm (ST02). Again the opening of the gap is almost parallel (see values position AF and BF in Table 2). Fatigue loading doubles the gap size in BoneLevel and a point contact was not seen at any measurement site.

Discussion

The results of this study show that a micro-gap exists in the investigated conical implant-abutment connections with or without load. Furthermore, fatigue loading increases this micro-gap in the systems evaluated.
Prior to the evaluation of the IAC under load application, the IAC´s were radiographed as received. All implant-abutment assemblies showed a continuous micro-gap with a minimum of 0.1 µm, with one implant-abutment assembly (AN) showing an exceptionally large micro-gap of up to 11 µm, this has also been verified previously using synchrotron based radio- and tomography. [24,25] The quantification of submicrometer gaps can be performed using synchrotron phase contrast radiography and numerical forward simulations of the optical Fresnel propagation. This allows the measurements of the microgap width down to 0.1 µm. [26]
A leakage-proof interface with surface contact between abutment and implant has long been proven not to exist.[10] This is due to the fact that the machining of metal parts leaves a certain surface roughness and surface geometry of the mating zone. While the geometries generated by designers in a technical drawing generally are smooth and straight, the real surface texture or topography of the workpiece is to a large extent determined by the formation of burrs and surface irregularities from the final milling process, therefore a surface contact is highly improbable in machined parts.[29] The imprecision of the implant-abutment connection has been documented in *in vitro* experiments [2,3] and the method to visualize the incongruence between the

implant and abutment in the mating zone has been described.[5] One virgin sample presented an exceptionally large micro-gap in the coronal portion of the implant-abutment interface prior to any load application, this might be based on the fact that the part is slightly out of specification; to elucidate the degree of fabrication tolerance the examination of more samples would be necessary.

Conical implant-abutment connections have become popular, as they have been proposed to have an enhanced mechanical stability during loading. [30] The mechanical stability has been calculated and shown through FE-Analysis [31] or measurements of the displacement of the abutment. [6,32] To date no data exist on the relation of the cone angle, the angle of load application and the mechanical stability of the abutment. This study shows that the flat conical connection (16°) shows higher stability (increase in micro-gap is smaller) to load applied in a 30° angle than the 5.7° conus, suggesting that the angle of the conical implant surface is decisive for the resistance to the application of load. A conical implant-abutment connection based on a 16° angled conus (ST) cannot be considered a self-locking connection, its mechanical features are rather similar to a butt-joint connection. This is concordance to the findings of a current study which shows that butt-joint connections seem to have a higher load bearing capacity against load applied in a 30° angle compared to conical connections with a smaller conus angle. [33] The length of the conus does not seem to influence the degree of micro-motion; it rather determines the mode of micro-gap formation. The annulling of the abutment when external force is applied is stopped by the abutment contacting the implant. The location of this contact depends on the angle of the conus and the extension of the abutment into the implant. In the flat angled implant this contact zone is below the mating zone (not captured within this study) leading to an almost parallel gap opening in the mating zone. Cyclic loading does not only decrease the mechanical stability of the implant-abutment connection, but also induces wear of the material. This has been shown in studies comparing different fatigue loading parameters [34,35] and materials used [36]. Individual parameters influence the wear behavior of the implant but to date this has not induced a change of the ISO Standard currently used to certify dental implants. Within this study fatigue loading has been performed by the Fraunhofer Institute in a standardized set-up in a dry environment and with a frequency of 15 Hz as proposed in the ISO Standard 14801:2003. When comparing the radiograph of the virgin and the fatigue-loaded smaller-diameter implant a massive plastic deformation of the

titanium and a fissure/crack at the implant-shoulder is evident besides an increase of the size of the micro-gap. The dimensions of the implant wall (0.4 mm) in this reduced diameter (3.5 mm) pure titanium (Grade 4) implant appears to be inadequate for cycling loading at a medium force (120 N). Plastic deformation of this implant type has been described to occur at 349 N in an experimental investigation under static overload at a diameter of 4.5 mm, suggesting that the thickness of the implant wall might also be of importance for the load-bearing capacity. [33] Synchrotron-based micro-tomography of IAC´s after fatigue loading has shown that there is essential material wear with plastic deformation of the titanium at the implant-abutment interface [24] at 120 N; albeit other reports suggesting only an elastic deformation at forces up to 600 N. [8,9] A lower frequency of load application is known to be a decisive factor of earlier fatigue failure of the implant, within this study the frequency was at medium range with excessive wear of the titanium implants as documented elsewhere. [35,24]

The fatigue loading protocol (120 N at an 30° angle) used within this study is a standard all implants need to pass to be certified. It comprises unidirectional loading on implants glued into a brass cylinder, which is not a physiological situation; multidirectional diverse forces would be more realistic on implants embedded in a material that has a similar elastic modulus as bone. As only two implants of each implant-abutment design has been used a statistical analyses cannot be performed within this pilot study. Currently a study has been initiated with a higher number of specimens and multi-directional load application to assess data in a more In-vivo-like situation. The data demonstrated within this study give an insight into the behavior of conical implant-abutment connections applying the ISO Standard 14801:2003.

Conclusion

This study demonstrates a detrimental impact of cyclic loading at medium force (120 N) on small-diameter implants. It also shows that the investigated conical IAC´s show a continuous micro-gap regardless of their design and the amount of force applied. The mechanical resistance of the abutment to micromotion seems to be related to the cone angle of the implant-abutment connection.

Acknowledgement

We would like to thank Dr. -Ing. M. Lengauer for the discussion and MDT Juergen Mehrhof for the sample preparation. T. Rack is a recipient of a doctorate grant from the Camlog Foundation. This study was partially funded by the German Research Association (DFG Nel 656/1-1 and ZA 656/1-1).

1. Binon P. Implants and components: entering the new millennium. Int. J. Oral Maxillofac. Implant 2000; 15: 76–95.
2. Semper W, Kraft S, Krüger T, Nelson K. Theoretical considerations: implant positional index design. J Dent Res 2009; 88: 725–730.
3. Semper W, Kraft S, Mehrhof J, Nelson K. Impact of abutment rotation and angulation on marginal fit: theoretical considerations. Int J Oral Maxillofac Impl 2010;25(4):752-8.
4. Binon PP, McHugh MJ The effect of eliminating implant/abutment rotational misfit on screw joint stability. Int J Prosthodont 1996;9(6):511-9.
5. Cibirka RM, Nelson SK, Lang BR, Rueggeberg FA. Examination of the implant-abutment interface after fatigue testing. J Prosthet Dent 2001;85(3):268-75.
6. Norton MR. In vitro evaluation of the strength of the conical implant-to-abutment joint in two commercially available implant systems. J Prosthet Dent 2000;83(5):567-71.
7. Cehreli MC, Akça K, Iplikçioğlu H, Sahin S. Dynamic fatigue resistance of implant-abutment junction in an internally notched morse-taper oral implant: influence of abutment design. Clin Oral Impl Res 2004;15(4):459-65.
8. Khraisat A, Baqain ZH, Smadi L, Nomura S, Miyakawa O, Elnasser Z. Abutment rotational displacement of external hexagon implant system under lateral cyclic loading. Clin Impl Dent Relat Res 2006;8(2):96-9.
9. Steinebrunner L, Wolfart S, Ludwig K, Kern M. Implant-abutment interface design affects fatigue and fracture strength of implants. Clin Oral Impl Res 2008;19: 1276-1284.
10. Jansen VK, Conrads G, Richter EJ. Microbial leakage and marginal fit of the implant-abutment interface. Int J Oral Maxillofac Implant 1997;12: 527–540.
11. Gross M, Abramovich I, Weiss EI. Microleakage at the abutment-implant interface of osseointegrated implants: a comparative study. Int J Oral Maxillofac Impl 1999;14(1):94-100.
12. Steinebrunner L, Wolfart S, Bösmann K, Kern M. In vitro evaluation of bacterial leakage along the implant-abutment interface of different implant systems. Int J Oral Maxillofac Impl 2005;20, 875–881.

13. Dibart S, Warbington M, Su MF, Skobe Z. In vitro evaluation of the implant-abutment bacterial seal: the locking taper system. Int J Oral Maxillofac Impl 2005;20(5):732-7.
14. Coelho PG, Sudack P, Suzuki M, Kurtz KS, Romanos GE, Silva NR. In vitro evaluation of the implant abutment connection sealing capability of different implant systems. J Oral Rehab 2008;35(12):917-24.
15. Harder S, Dimaczek B, Açil Y, Terheyden H, Freitag-Wolf S, Kern M. Molecular leakage at implant-abutment connection--in vitro investigation of tightness of internal conical implant-abutment connections against endotoxin penetration. Clin Oral Investig 2010;14(4):427-32.
16. Aloise JP, Curcio R, Laporta MZ, Rossi L, da Silva AM, Rapoport A. Microbial leakage through the implant-abutment interface of Morse taper implants in vitro. Clin Oral Impl Res 2010;21(3):328-35.
17. Nedir R, Bischof M, Szmukler-Moncler S, Belser UC, Samson J. Prosthetic complications with dental implants: from an up-to-8-year experience in private practice. Int J Oral Maxillofac Impl 2006;21(6):919-28.
18. Jung RE, Pjetursson BE, Glauser R, Zembic A, Zwahlen M, Lang NP. A systematic review of the 5-year survival and complication rates of implant-supported single crowns. Clin Oral Impl Res 2008;19(2):119-30.
19. Bozini T, Petridis H, Garefis K, Garefis P. A meta-analysis of prosthodontic complication rates of implant-supported fixed dental prostheses in edentulous patients after an observation period of at least 5 years. Int J Oral Maxillofac Impl 2011;26(2):304-18.
20. Duyck J, Van Oosterwyck H, Vander Sloten J, De Cooman M, Puers R, Naert I. Magnitude and distribution of occlusal forces on oral implants supporting fixed prostheses: an in vivo study. Clin Oral Impl Res 2000;11(5):465-75.
21. Mericske-Stern R, Geering AH, Buergin W. Three-dimensional force measurements on mandibular implants supporting overdentures. Int J Oral Maxillofac Impl 1992;7: 185–194.
22. Morneburg T, Proeschel PA. Measurement of masticatory forces and implant loads: a methodologic clinical study. Int J Prosthodont 2002 ;15 : 20–7.
23. Standardization. International Standard ISO 14801 – dentistry – implants-dynamic fatigue test for endosseous dental implants. Geneva: International Organization for Standardization; 2007.

24. Zabler S, Rack T, Rack A, Nelson K. Fatigue induced deformation of taper connections in dental titanium implants. Int J Mat Res 2012; 103:207-16
25. Rack A, Rack T, Stiller M, Riesemeier H, Zabler S, Nelson K. Journal of Synchrotron Radiation 2010;17(2): 289-294
26. Zabler S, Rack T, Rack A, Nelson K. Quantitative studies on inner interfaces in conical metal joints using hard X-ray inline phase contrast radiography. Rev Sci Instr ;81(10): 103703
27. Banhart J. Advanced Tomographic methods in material research and engineering. Oxford University Press; 2008
28. Stock SR. Synchrotron microComputed Tomography of the mature bovine dentinoenamel junction. J Struct Biol 2008;161(2):144-50.
29. Burrs P. Analysis, control and removal. CIRP Ann Man Tech 2009;58:519–542
30. Bozkaya D, Müftü S. Efficiency considerations for the purely tapered interference fit (TIF) abutments used in dental implants. J Biomech Eng 2004;126(4):393-401.
31. Akça K, Cehreli MC. Evaluation of the mechanical characteristics of the implant-abutment complex of a reduced-diameter morse-taper implant. A nonlinear finite element stress analysis. Clin Oral Impl Res 2003 ;14 : 444–54.
32. Meng JC, Everts JE, Qian F, Gratton DG. Influence of connection geometry on dynamic micromotion at the implant-abutment interface. Int J Prosthodont 2007;20(6):623-5.
33. Dittmer S, Dittmer M, Kohorst P, Jendras M, Borchers L, Stiesch M. Effect of implant-abutment connection design on load bearing capacity and failure mode of implants. J Prosthodont 2011 ;20(7):510-6
34. Cornell KL, Karl M, Kelly RJ. Evaluation of test protocol variables for dental implant fatigue research. Dent Mat 2009 ; 25 : 1419-25
35. Karl M, Kelly RJ. Influence of loading frequecy on implant failure under cyclic fatigue conditions. Dent Mat 2009 ; 25 :1426-32
36. Klotz MW, Taylor TD, Goldberg AJ. Wear at the titanium-zirconia implant-abutment Interface : A Pilot Study. Int J Oral Maxillofac Impl 2011 ; 26 :970-75

Table 1 Details of the implant-abutment assemblies used (V: virgin, F: fatigue loaded)

Abbreviation	System	Manu-facturer	Standardized characteristics of implants and abutments	Dimensions of implant and IAC · [mm] / L [mm]	Angle of cone (°)	Length of mating zone (mm)
AN01 (V) AN02 (F)	Ankylos c/x	Friadent	Implant: REF: 17-0546/31010420, LOT: 0020035388 Abutment: REF: 31024140 LOT: 20035853	Implant: 3.5 / 14; IAC: 2.5 / 1.8	5.7	1.82
ANP01 (V) ANP02 (F)	Ankylos plus	Friadent	Implant: REF: 31010220, LOT: 20037235 Abutment: REF: 31024180 LOT: 20035821	Implant: 3.5 / 14 IAC: 2.5 / 2.2	5.7	2.01
ST01 (V) ST02 (F)	Bonelevel	Straumann AG, Basel, Switzerland	Implant: REF: 021.4114, LOT: G6582 Abutment: REF:	Implant: 4.1 / 14.2 IAC: 3.3 / 0.7	16	0.76

			022.2202 LOT: F6601			

Table 2 Size of microgap under different mechanical load conditions

System	Gap size in µm															
	0 N				30 N, 90°				100 N, 90°				200 N, 30°			
	virgin		fatigue loaded		virgin		fatigue loaded		virgin		fatigue loaded		virgin		fatigue loaded	
Ankylos c/x (AN)	11	*0.6*	4	*0.7*	0.2	*12*	0.5	*12*	0.5	*28*	1.2	*24*	0.1	*24*	0.1	*22*
	0.3	*0.1*	0.2	*0.1*	0.9	*0.1*	0.7	*0.2*	4.6	*0.1*	2.5	*0.2*	0.7	*0.1*	3	*0.1*
Ankylos plus (ANP)	0.3	*0.2*	31	*5*	0.6	*3*	1	*32*	3	*18.5*	0	*36*	0.1	*9*	-	*25*
	0.2	*0.3*	1	*3*	1.2	*0.2*	12	*0.3*	10	*0.1*	30	*0*	4	*0.1*	-	*0.1*
Straumann (ST)	0.2	*0.2*	0.8	*0.7*		*4*		*1.8*		*14*		*18*	0.2	*0.3*	0.3	*1*
	0.4	*0.3*	0.2	*0.7*		*4*		*1.7*		*10*		*13*	0.3	*0.6*	0.1	*1*

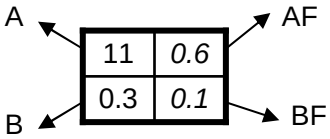

Assignment of the values in the table with respect to the positions as defined in Fig. 1.

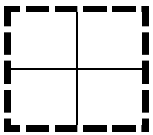

Horizontal loading values for virgin IAC described in Rack et al., 2010

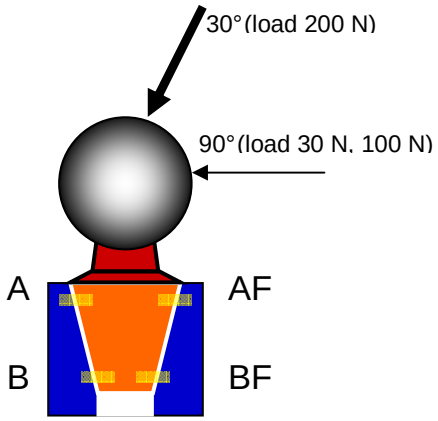

Figure 1. Schematic illustration of positions of extracted profiles (yellow) with the direction and values of static load application (grey: steel ball glued onto abutment according to DIN ISO 14801; orange: rotation safe abutment torque tightened to the implant body (blue); yellow: area of measurement as described (Zabler et al., 2010).

2a

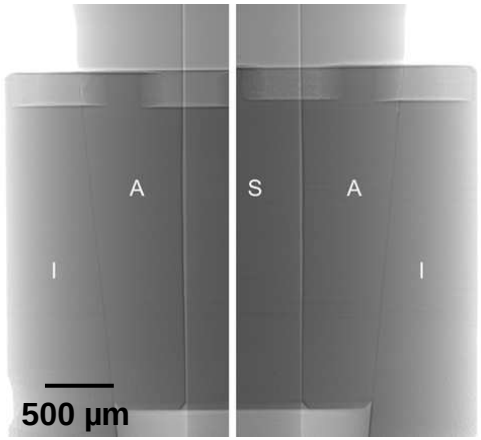

2b

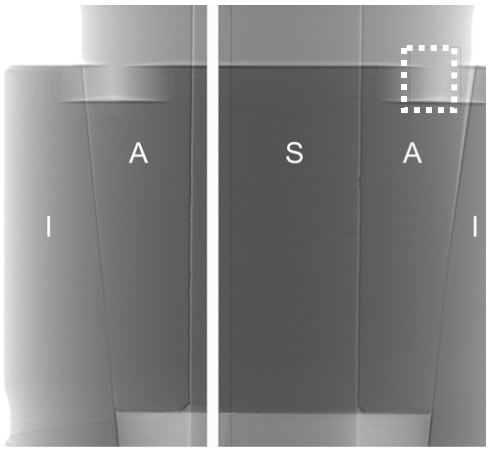

2c

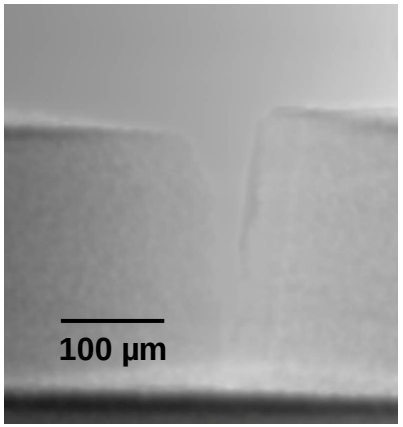

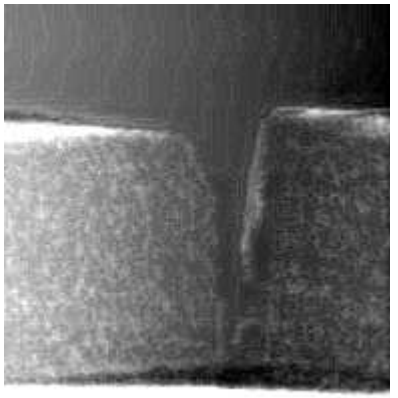

Figure 2. Radiographs of Ankylos plus IAC without mechanical static load (0 N). I – implant, A – abutment, S – screw.

2a – Ankylos plus (ANP01) before fatigue loading (V).

2b – Ankylos plus (ANP02) after fatigue loading (F), the marked region is depicted in Fig 2.c.

2c – Fissure in the coronal portion of implant (left: original image, right: edge enhanced image).

3a

3b

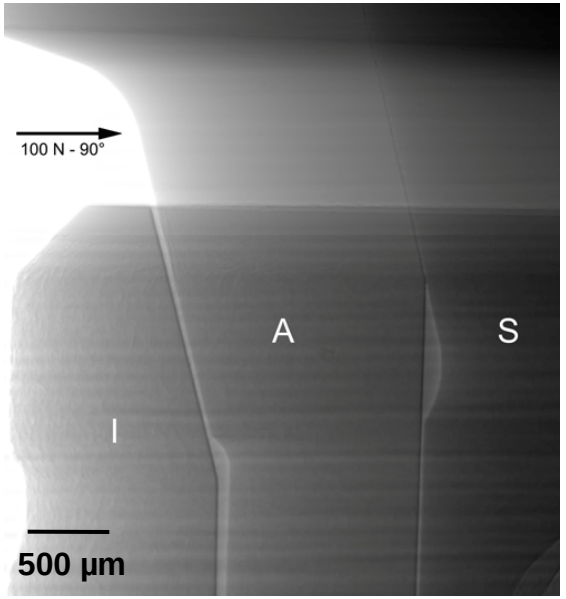

Figure 3. Radiographic images of fatigue loaded Ankylos plus IAC (ANP02) – 3a, and fatigue loaded Straumann BoneLevel (ST02) – 3b under static horizontal load of 100 N. I – implant, A – abutment, S – screw.

4a

b

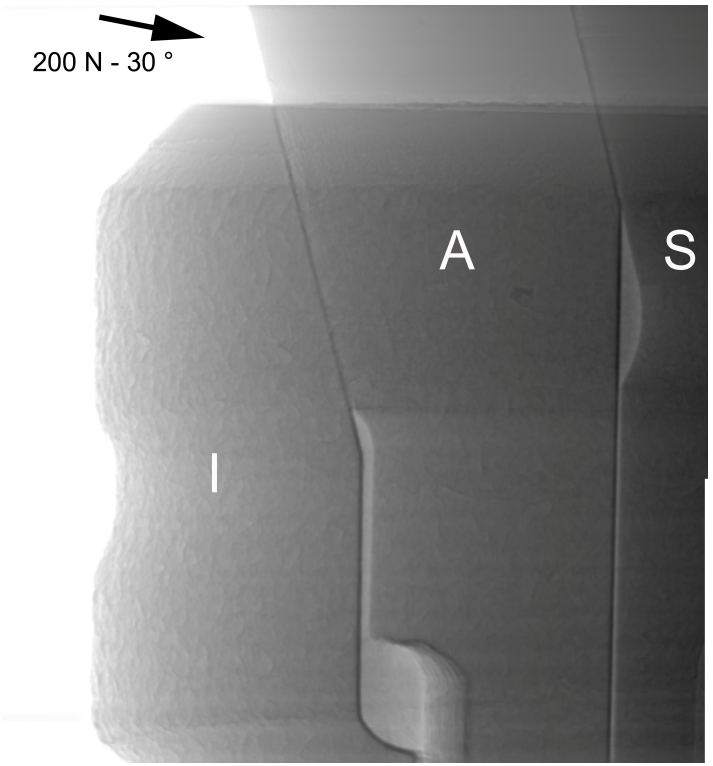

Figure 4. Radiographic images of virgin Ankylos c/x IAC (AN01) – 4a, and fatigue loaded Straumann BoneLevel (ST02) – 4b under static load of 200 N in a 30 ° angle. I – implant, A – abutment, S – screw.